

Electromagnetic modelling of HTS tapes using Gmsh/GetDP

F. Trillaud¹, P. Kis², C.S. López-Monsalvo³, R. Escarela-Pérez³, C. Geuzaine⁴

¹Instituto de Ingeniería, Universidad Nacional Autónoma de México, CDMX, 04510 Mexico

²Furukawa Electric Institute of Technology Ltd., Kesmark u. 28/A, 1158 Budapest, Hungary

³Universidad Autónoma Metropolitana (Azcapotzalco), CDMX, 02200 Mexico

⁴University of Liege, Montefiore Institute B28, Sart Tilman campus, B-4000 Liege, Belgium

June 16, 2016

Overview

- 1 Introduction
- 2 Mixed nodal and edge elements
- 3 Examples with Onelab
- 4 **h**-formulation and weak form
- 5 Homology and cohomology
- 6 Implementation of model in Onelab: template
- 7 Results
- 8 Conclusion
- 9 References

Introduction

The main goal of this presentation is threefold:

- Laying out the mixed nodal and edge element method in electromagnetism
- Showing its implementation in the open source software Onelab combining the modeller Gmsh and the FEM solver GetDP
- Give a "light" introduction to homology and cohomology and how it is resolved in Gmsh (first de Rham's cohomology group)

A benchmark and a case study are presented as practical examples: a) one single HTS tape with AC transport current (benchmark 1), b) a solenoidal coil made of commercial (Re)BCO wires with a ramped transport current. The results of Onelab were compared to COMSOL Multiphysics[®] and Norris's formula in the simplest case a).

N.B.: To understand the implementation in Onelab, notions of topology and differential geometry are required and in particular the significance of the homology and cohomology groups leading to the homology and cohomology functions in Gmsh and for the latter its connection to the FEM solver GetDP.

Mixed nodal and edge finite elements [1, 2]

The nodal finite elements have been widely used in mechanics and thermal analysis and were mainstreamed in electromagnetism before the venue of the edge elements. The following gives a brief overview of typical features of those elements.

The nodal elements ensure the continuity of all components from elements to elements (leads to complication when discontinuities of fields must be taken into account across different media). 3 unknown per nodes and an error of second order.

The edge elements represent the circulation of the vector field solution along edges of the mesh ensuring the continuity of its tangent component from elements to elements (allowing discontinuity of the normal component). It is nowadays the preferred choice to model electromagnetic systems. One unknown per edge of the element (6 in a tetrahedron), error of first order. Whitney 1 elements are free of divergence (very useful for divergence free solution). Edge elements are more sensitive to the quality of the mesh (shape of the triangles).

Mixing nodal and edge elements leads to a smaller linear system to work with (more zero entries in the rigidity matrix) with lesser singularities with a lower number of degrees of freedom (storage and computational time).

Benchmark 1 and (Re)BCO pancake

Benchmark 1: one single tape with AC transport current at 50 Hz

- 1 A single tape having thickness of $1 \mu\text{m}$ and a width of 12 mm
- 2 $I_c = 300 \text{ A}$, $h/I_c = \{0.1, 0.2, \dots, 0.9\}$ and $n = \{25, 101\}$

Case study (work in progress): one pancake coil made of 20 commercial (Re)BCO tapes connected in series with a ramped transport current

- 1 Commercial tape having thickness of $1 \mu\text{m}$ and stabilised by Cu ($40 \mu\text{m}$ thick) and a width of 4 mm
- 2 $I_c = 100 \text{ A}$, and $n = 38$

Power law model: resistivity of the HTS tape

$$\rho = \frac{E_c}{J_c^n} J_t^n, \quad J_c = \text{cst}, \quad n = \text{cst}, \quad E_c = 1 \mu\text{V/cm}$$

Single tape and pancake coil

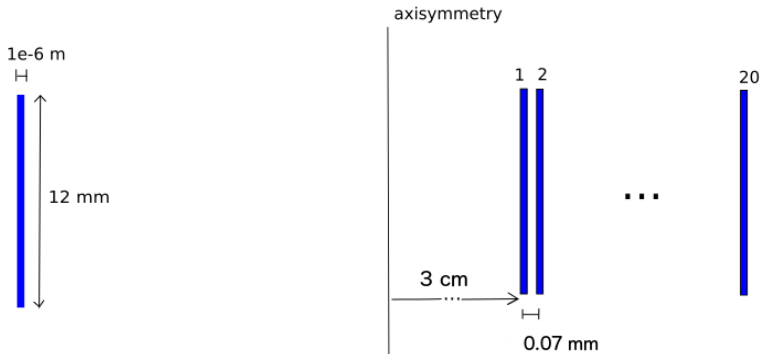


Figure: Left: single HTS tape (benchmark 1, 12 mm wide). Right: pancake coil made of 20 commercial YBCO tapes connected in series (4 mm wide).

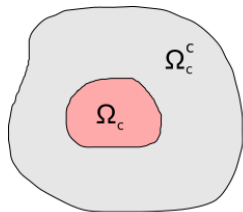
h-formulation

From the Maxwell-Ampère equations $\nabla \times \mathbf{h} = \mathbf{j}$ and the constitutive laws, $\mathbf{b} = \mu \mathbf{h}$, $\mathbf{e} = \rho \mathbf{j}$, one can derive the following **h**-formulation directly from the Maxwell-Faraday equation, $\nabla \times \mathbf{e} = -\partial_t \mathbf{b}$, leading to,

$$\nabla \times [\rho \nabla \times \mathbf{h}] + \partial_t (\mu \mathbf{h}) = 0, \quad (1)$$

which is valid over the entire domain Ω .

$\text{div}(\mathbf{b}) = 0$ is ensured by setting $\mathbf{b}(t = 0) = 0$ [3].



$$\Omega = \Omega_c \cup \Omega_c^c$$

Figure: Definition of the domains, Ω_c : conductor, Ω_c^c : surrounding (complementary subspace).

Weak formulation

From the PDE (1), the following expression is derived over the entire domain Ω for any test functions \mathbf{v} ,

$$\int_{\Omega_c} (\nabla \times [\rho \nabla \times \mathbf{h}] \cdot \mathbf{v}) + \int_{\Omega} (\partial_t(\mu \mathbf{h}) \cdot \mathbf{v}) = 0, \quad \forall \mathbf{v} \in F(\Omega)$$

where F is the space of test functions defined on Ω .

Using Green's formula, one can lower the order of differentiation of the previous equation,

$$\int_{\Omega_c} (\rho \nabla \times \mathbf{h}) \cdot (\nabla \times \mathbf{v}) + \int_{\Omega} \partial_t(\mu \mathbf{h}) \cdot \mathbf{v} = - \int_{\Omega_c} (\mathbf{n} \times \mathbf{e}) \cdot \mathbf{v}, \quad (2)$$

where $\partial\Omega_c$ is the boundary of Ω_c and $\mathbf{e} = \rho \nabla \times \mathbf{h}$. Without considering the negative sign, the right hand side is the expression of the source voltage \mathcal{V} in the weak sense.

"Light" presentation of homology and cohomology in the frame of differential geometry [4, 5]

Generalised Stokes theorem on manifolds ("fundamental" theorem of multivariable calculus)

$$\int_{\Omega} d\omega = \int_{\partial\Omega} \omega, \text{ or } \langle \Omega, d\omega \rangle = \langle \partial\Omega, \omega \rangle \quad (3)$$

where ω is a differential form defined on a differentiable manifold Ω (topological space locally resembling an Euclidean space on which one can define global differential forms). d is the exterior derivative dual to the ∂ being the boundary operator.

Some examples: $\iint_{\Omega} \nabla \times \mathbf{e} \cdot \mathbf{n} = \oint_{\partial\Omega} \mathbf{e} \cdot \mathbf{t}$ (\mathbf{e} is 1-form), and $\iiint_{\Omega} \nabla \cdot \mathbf{d} = \iint_{\partial\Omega} \mathbf{d} \cdot \mathbf{n}$, $\Omega \subset \mathbb{R}^3$ (\mathbf{d} is a 2-form).

Poincaré lemma

The Poincaré lemma states that a closed form defined on a contractible open subset of \mathbb{R}^n is exact ($d\omega = 0 \Leftrightarrow \omega = d\eta$). It is the basis to find cosets of closed forms representing cohomology classes.

Homology and cohomology groups

Homology tries to answer the following question, "how can we identify holes in a geometric structure?". The 1-homology group $H_1(\Omega)$ of primary interest in \mathbb{R}^3 is generated by the class of curves that enclose a "hole" in Ω .

Cohomology represents the class of closed differential forms ($d\omega = 0$) which are not exact on cycles (closed chains) meaning that ω is not the differential form of any potential function ($\omega \neq d\eta$). The 1-cohomology group, written as $H^1(\Omega)$, is equivalent to the corresponding homology group according to de Rham's isomorphism (a class of closed differential forms not-exact is paired to a class of generators of $H_1(\Omega)$ and conversely). Poincaré lemma and Stokes theorem (3) are key elements to define the classes of $H^p(\Omega)$.

Duality homology and cohomology and de Rham's isomorphism [5]

Homology	Cohomology
$\partial_p \partial_{p+1} = 0$	$d^p d^{p-1} = 0$
$\text{Im}(\partial_{p+1}) \subset \ker(\partial_p)$	$\text{Im}(d^{p-1}) \subset \ker(d^p)$
$H_p = \ker(\partial_p) / \text{Im}(\partial_{p+1})$	$H^p = \ker(d^p) / \text{Im}(d^{p-1})$
Classes of closed p chains (p cycles) that are not boundary of $p+1$ chain	Classes of closed differential forms (p co-chains) that are not exact meaning they are not the <i>co-boundary</i> of a $p-1$ co-chains
$\langle \partial_p \partial_{p+1} \Omega, \omega \rangle = \langle \partial_{p+1} \Omega, d^{p-1} \omega \rangle = \langle \Omega, d^p d^{p-1} \omega \rangle = 0$	
All exact forms are closed. On a simply connected finite space, all closed forms are exact.	
de Rham's isomorphism:	
$H_p(\Omega) \sim H^p(\Omega)$ for all p , $\beta_p = \dim(H_p) = \dim(H^p)$ (Betti number or rank)	

Simply connected domain and notion of cut

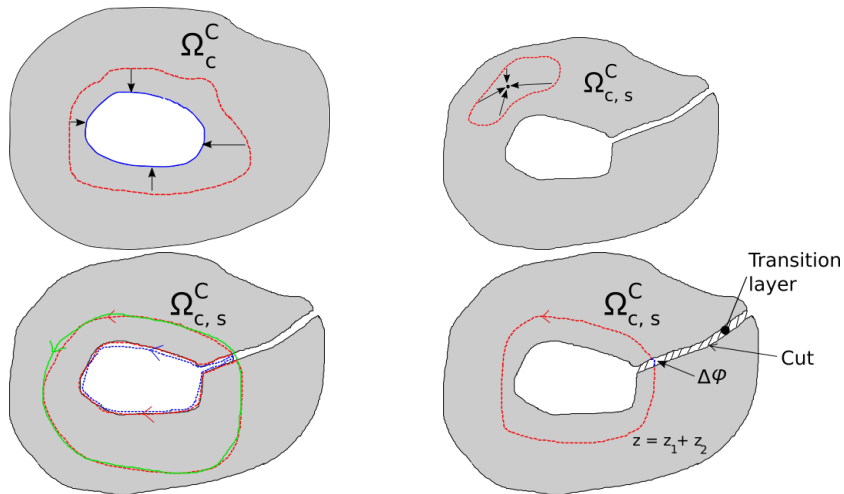


Figure: Upper left: domain not simply connected. Upper right: simply connected domain. Lower left: cycle z_1 -red over the simply connected domain and z_2 -blue which is not a boundary of any domain, making the green circulation $z_1 + z_2$ over the multiply connected domain. Lower right: the composition of the circulations and the basic concept of a cut over which one can associate a discontinuous potential function ϕ .

Homology and cohomology in Gmsh [6, 7]

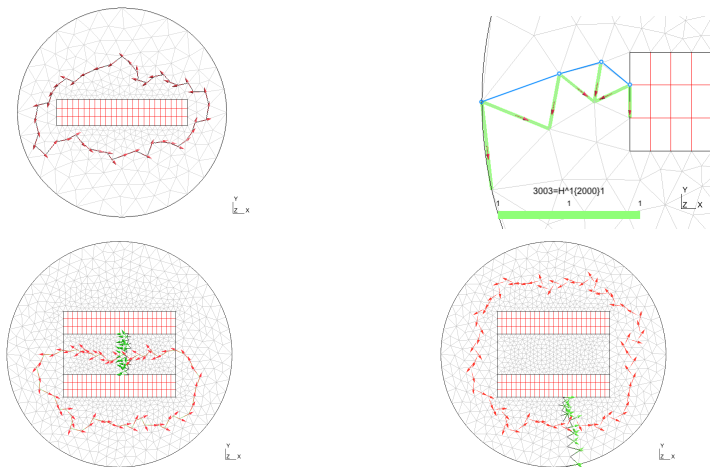


Figure: Upper figures show the mesh used to solve the benchmark 1. Upper left: generator of the homology group $H_1(\Omega)$, $\beta_1 = 1$ leading to a single cut. Upper right: "equivalent" edge element basis functions of the cohomology group $H^1(\Omega)$ (red arrows in the upper right mesh), the cut is outlined in blue color. Lower: model with 2 conductors for which the generators are shown along with the corresponding cuts ($\beta_1 = 2$, 2 cuts).

Computation of generators of H_1 as well as the the cuts. Their basis functions from H^1 are associated in GetDP.

```
Cohomology(1){{Omega_CC_ID}, {}}; % 1-cohomology group: H^1  
Homology(1){{Omega_CC_ID}, {}}; % 1-homology group: H_1
```

The cuts have been created and are identified as an unitary increment of the domain identifier (integer) "Omega_CC_ID". It remains to associate the global term to the basis functions over the cut in GetDP. The "Homology(){}{}" function allows to create a generator of the coset of H_1 .

Basis and test functions [8, 9, 2]

GetDP uses the Galerkin method for which the test functions \mathbf{v} are chosen in the same space than the basis functions. The basis functions are polynomial functions that interpolate the solution over the mesh, see (4).

In the mixed nodal and edge element discretization of the problem where the edge elements are naturally associated with the conductive region Ω_c and the nodal elements to the complementary space Ω_c^C , the magnetic field \mathbf{h} can be decomposed as follows,

$$\mathbf{h} = \sum_{e \in E_c} h_e \mathbf{s}_e + \sum_{n \in N_c^C} \Phi_n \mathbf{v}_n + \sum_{i \in C_i} \mathcal{I}_i \mathbf{c}_i \quad (4)$$

where \mathbf{s}_e are edge element basis functions belonging to the inner edges of Ω_c , $\mathbf{v}_n = -\nabla(s_n)$ a gradient of a continuous scalar function defined over the simply connected $\Omega_{c,s}^C$ (Ω_c^C without the cuts C_i) and $\mathbf{c}_i = -\sum_{n \in N_{c,c}^C} \nabla(q_n)$ the sum of gradients of scalar functions ("global quantity") discontinuous over

the cut C_i (transition layer over which $0 \leq q_n \leq 1$, and $q_n = 0$ otherwise). N_c^C are the nodes of Ω_c^C including the boundary $\partial\Omega_c$. $N_{c,c}^C$ are the nodes belonging to the cut and connecting nodes of the transition layer.

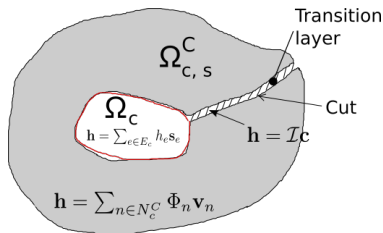


Figure: Distribution of the functions.

Example: benchmark 1

For a single conductor, the weak formulation (2) yields,

$$\int_{\Omega_c} (\rho \nabla \times \mathbf{h}) \cdot (\nabla \times \mathbf{v}) + \int_{\Omega} \partial_t (\mu \mathbf{h}) \cdot \mathbf{v} = -\mathcal{V}, \quad (5)$$

where the voltage \mathcal{V} is zero almost everywhere on a close path excepting where the boundary of the conductor meets the cut.

In contrary to the voltage, the current \mathcal{I} through the Maxwell-Ampère equation, $\oint_z \mathbf{h} = \mathcal{I}$ where z any cycles of H_1 , must be enforced. The corresponding basis functions \mathbf{c} to which \mathcal{I} is associated is generated by GetDP and associated with edge elements in the transition layer at the cut.

It should be noted that the definition of both voltage and current leads to a unique solution of the magnetic field over the domain Ω .

Global quantity: voltage \mathcal{V}

To unveil the voltage \mathcal{V} , the left hand side of equation (2) should be rearranged,

$$\int_{\partial\Omega_c} (\mathbf{n} \times \mathbf{e}) \cdot \mathbf{v} = \int_{\partial\Omega_c} (\mathbf{v} \times \mathbf{e}) \cdot \mathbf{n} = - \int_{\partial\Omega_c} (\nabla(q) \times \mathbf{e}) \cdot \mathbf{n} = \int_{\partial\Omega_c} (\nabla \times (q\mathbf{e})) \cdot \mathbf{n} - \int_{\partial\Omega_c} q(\nabla \times \mathbf{e}) \cdot \mathbf{n}.$$

Since $\int_{\partial\Omega_c} q(\nabla \times \mathbf{e}) \cdot \mathbf{n} = - \int_{\partial\Omega_c} \partial_t \mathbf{b} \cdot \mathbf{n} = 0$ (imposing $\mathbf{b} \cdot \mathbf{n} = 0$ over $\partial\Omega_c$).

Therefore,

$$\int_{\partial\Omega_c} (\mathbf{n} \times \mathbf{e}) \cdot \mathbf{v} = \int_{\partial\Omega_c} (\nabla \times (q\mathbf{e})) \cdot \mathbf{n} = \int_{\partial\Omega_c} q\mathbf{e} = \int_{\partial\Omega_c \cap C} \mathbf{e} = \mathcal{V},$$

across the cut where $\partial\Omega_c \cap C$ where $q = 1$ [10].

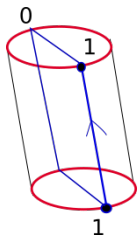


Figure: Integration over $\partial\Omega_c \cap C$.

Global quantity: current \mathcal{I}

The Ampère's law is strongly satisfied owing to the creation of a cut changing a multiply connected domain Ω into the union of simply connected domains Ω_c and Ω_c^C .

In the simply connected domain $\Omega_{c,s}^C$ (s stands for simply connected), one can define a single continuous scalar potential function ϕ so that $\mathbf{h} = -\nabla(\phi)$ be represented as nodal functions. Indeed, on single connected domains, all closed forms are exact and therefore $\oint_c \mathbf{h} = 0$ for any closed loops c in $\Omega_{c,s}^C$.

Through the cut, one defines a discontinuous potential functions and fixes the global quantity as the transport current thereby enforcing the Ampère's law ¹. Using (4) over a cycle z of the 1-homology group H_1 , one can show that,

$$\int_z \mathbf{h} = \int_{z^*} \mathbf{h} = \phi_1 - \phi_2 = \phi_1 = \mathcal{I},$$

z^* , the portion of z belonging to the transition layer.

¹ Be aware that for more than one conductor, it is important to apply the cohomology solver to each separated conductor to associate the produced cut later on with its corresponding global quantity. Indeed, if the generator of H_1 enlases N conductors, the circulation of the magnetic field over it according to Ampère's law is equal to $N\mathcal{I}$.

Linearization and implementation: part 1

From the Weak formulation, we got the following,

$$\int_{\Omega_c} (\rho \nabla \times \mathbf{h}) \cdot (\nabla \times \mathbf{v}) + \int_{\Omega} \partial_t (\mu \mathbf{h}) \cdot \mathbf{v} = 0,$$

where ρ is a function of $\nabla \times \mathbf{h}$ (nonlinear term). Using an iterative scheme, let's recall that the k^{th} iteration leads to,

$$\int_{\Omega_c} \mathbf{e}_k \cdot (\nabla \times \mathbf{v}) + \int_{\Omega} \partial_t (\mu \mathbf{h}_k) \cdot \mathbf{v} = 0,$$

where $\mathbf{e}_k = \mathbf{e}_{k-1} + \delta \mathbf{e} = \mathbf{e}_{k-1} + \left. \frac{d\mathbf{e}}{d\mathbf{j}} \right|_{k-1} \delta \mathbf{j}$. To improve the convergence, one may use a relaxation technique so that $\delta \mathbf{j} = \alpha_k (\mathbf{j}_k - \mathbf{j}_{k-1})$ where α_k is the relaxation factor at the current iteration ². Hence, one can re-express (6) as follows,

$$\int_{\Omega_c} (\rho_{k-1} \nabla \times \mathbf{h}_{k-1}) \cdot (\nabla \times \mathbf{v}) + \int_{\Omega_c} \alpha_k \left. \frac{d\mathbf{e}}{d\mathbf{j}} \right|_{k-1} (\nabla \times \mathbf{h}_k) \cdot (\nabla \times \mathbf{v}) - \int_{\Omega_c} \alpha_k \left. \frac{d\mathbf{e}}{d\mathbf{j}} \right|_{k-1} (\nabla \times \mathbf{h}_{k-1}) \cdot (\nabla \times \mathbf{v}) + \dots$$
$$\dots \int_{\Omega} \partial_t (\mu \mathbf{h}_k) \cdot \mathbf{v} = 0,$$

²scheme proposed by C. Geuzaine in the model titled "superconductors" available with the latest distribution of Onelab

Linearization and implementation: part 2

The time derivative is handled by a Backward Euler's scheme ($\theta = 1$ in the θ -scheme) [11],

$$\partial_t(\mu \mathbf{h}_k) \simeq \mu \left(\frac{\mathbf{h}_k^{t+\delta t} - \mathbf{h}_k^t}{\delta t} \right) = \theta \mathbf{f}(\mathbf{h}_k^{t+\delta t}, t + \delta t) + (1 - \theta) \mathbf{f}(\mathbf{h}_k^t, t) = \mathbf{f}(\mathbf{h}_k^{t+\delta t}, t + \delta t),$$

where δt is the chosen time step and the permeability μ is assumed constant.

The Jacobian matrix $\frac{d\mathbf{e}}{d\mathbf{j}}$ is expressed as,

$$\frac{d\mathbf{e}}{d\mathbf{j}} = \rho \mathbb{I}_3 + \frac{1}{j} \frac{\partial \rho}{\partial j} (\mathbf{j}\mathbf{j}^t),$$

where ρ is the isotropic resistivity, \mathbb{I}_3 is the Identity matrix (3x3), $\mathbf{j}\mathbf{j}^t$ the product of \mathbf{j} (3x1) and its transpose (1x3), and $j = \|\mathbf{j}\|_2$.

The boundary coupling between the nodal and edge finite elements at the frontier of the two is ensured by the conservation of the circulation,

$$h_{1-2} = \int_{\mathbf{e}_{1-2}} \mathbf{h} = \int_1^2 -\nabla(\phi) = - \int_{\phi_1}^{\phi_2} d\phi = \phi_1 - \phi_2.$$

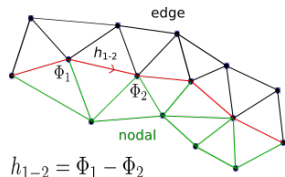


Figure: Boundary continuity between nodal and edge finite element domains.

GetDP code: test and basis functions

In the shape of GetDP code.

Block: "FunctionSpace"

```
{
  {Name H_FunctionSpace; Type Form1;
   BasisFunction
   {
     {Name h_Edge; NameOfCoef s_Edge; Function BF_Edge;
      Support Omega.c; Entity EdgesOf[All, Not nodalEdgeBoundaryRegion];}
     {Name h_Node; NameOfCoef v_Node; Function BF_GradNode;
      Support Omega; Entity NodesOf[nodalRegion];}
     {Name l_Edge; NameOfCoef c_Edge; Function BF_GroupOfEdges;
      Support Omega; Entity GroupsOfEdgesOf[cut];}
   }
  GlobalQuantity
  {
    {Name I1; Type AliasOf; NameOfCoef c_Edge;}
    {Name V1; Type AssociatedWith; NameOfCoef c_Edge;}
  }
  Constraint
  {
    {NameOfCoef I1; EntityType GroupsOfEdgesOf; NameOfConstraint currentConstraint;}
    {NameOfCoef V1; EntityType GroupsOfEdgesOf; NameOfConstraint voltageConstraint;}
  }
}
```

Type "Form1" or curl-conform. The "currentConstraint" and the "voltageConstraint" have been set previously. In the present case, the "voltageConstraint" is empty since it is part of the weak form of the problem (see equation (5)) being resolved over the cut.

GetDP code: weak formulation

In the shape of GetDP code.

Block: "Formulation"

```
...
Equation{
  Galerkin{
    [rho[{\d H}]*{\d H}, {\d H}]; In Omega.c;
    Jacobian jacobianTransformation; Integration basicIntegration;}
  Galerkin{
    [$alpha*dEdJ[{\d H}]*Dof{\d H}, {\d H}]; In Omega.c;
    Jacobian jacobianTransformation; Integration basicIntegration;}
  Galerkin{
    [-$alpha*dEdJ[{\d H}]*{\d H}, {\d H}]; In Omega.c;
    Jacobian jacobianTransformation; Integration basicIntegration;}
  Galerkin{
    DtDof[mu0*Dof{H}, {H}]; In Omega;
    Jacobian jacobianTransformation; Integration basicIntegration;}
  GlobalTerm{
    [Dof{V1}, {I1}]; In cut;}}
...
```

where $Dof\{d h\}$ is the current iteration (Dof for degree of freedom) to be computed or $\nabla \times h_k$ and $\{d h\}$ is the result from the past iteration or $\nabla \times h_{k-1}$.

GetDP code: resolution

Block: "Resolution"

```
SaveSolution[H.System];
Evaluate[$alpha = 1];
TimeLoopTheta[initialTime , finalTime , timeStep , theta]
{
  Generate[H.System];
  Solve[H.System];
  Generate[H.System];
  GetResidual[H.System, $initialResidual];
  Evaluate[$residual = $initialResidual, $ii = 0];
  Print[{ $ii, $residual, $residual/$initialResidual},
    Format "Residual %3g - absolute value: %2.9g; relative value: %2.9g"];
  While[((( $residual > absoluteTolerance) && ($residual/$initialResidual > relativeTolerance)
    && ($ii < maximumNumberOfIterations))]
  {
    Solve[H.System];
    Generate[H.System];
    GetResidual[H.System, $residual];
    Evaluate[$ii = $ii+1];
    Print[{ $ii, $residual, $residual/$initialResidual},
      Format "Residual %3g - absolute value: %2.9g; relative value: %2.9g"];
  }
  SaveSolution[H.System];
}
```

Galerkin method: minimisation of weighted residual $R(\mathbf{h}_{jk})$ ($R = \nabla \times [\rho \nabla \times \tilde{h}] + \partial_t (\mu \tilde{h})$, with \tilde{h} the approximated numerical solution) [12].

Results: single tape AC losses (12 mm x 1 μm , benchmark 1)

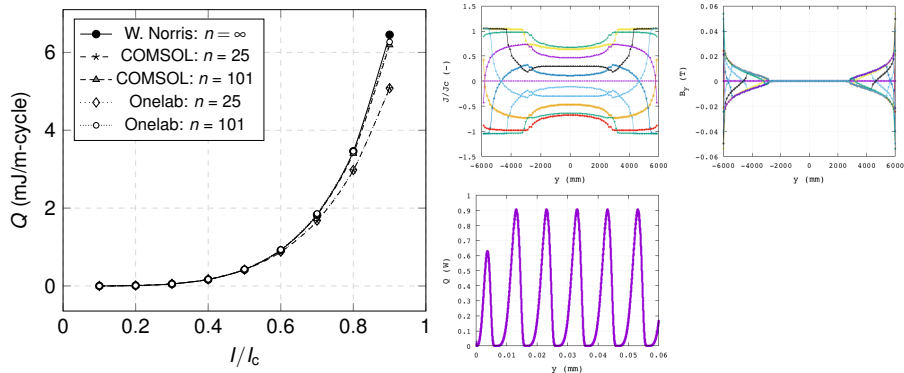


Figure: Left: AC losses of a single tape (1 μm thick and 12 mm wide) for different fractions of transport current at two n -values (25 and 101) and the comparison with Norris' formula and COMSOL Multiphysics[®]. Right: detail of the results at $0.9I_c$ and $n = 101$. Computational time ranging from roughly 2 min. ($n = 25$ to 2 hrs for $n = 101$ at $0.9I_c$), to span 3 cycles. The results are less than a fraction of percent comparable to COMSOL Multiphysics[®].

Results: (Re)BCO pancake, 20 commercial tapes 1/1

- 1 The coil is made from SCS4050 (20 μm Cu on both sides, 2 μm Ag, 1 μm YBCO and 50 μm Ha for a 4 mm wide tape).
- 2 Air gap between the turns is 0.07 mm
- 3 $E_c = 1\text{e-}4$ V/m, $I_c = 100$ A, $n = 38$
- 4 Current ramped at 1000 A/s up to 100 A

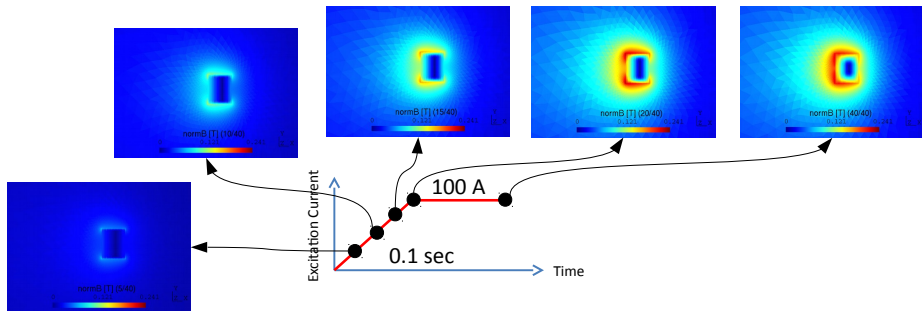


Figure: Ramping up of the current in the magnet, distribution of magnetic field. Running time is 20 min on a single core of Intel(R) Core(TM) i5-2410M CPU @ 2.30GHz.

Results: (Re)BCO pancake, 20 commercial tapes 1/2

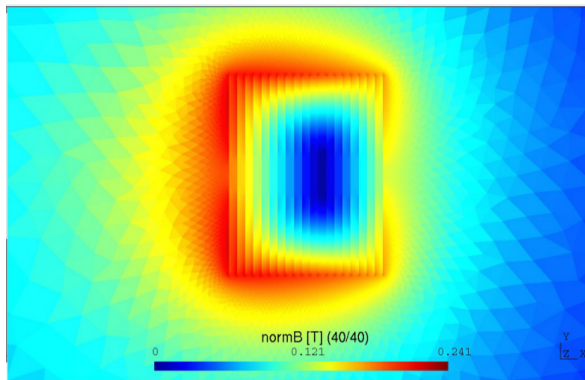


Figure: Magnetic flux density distribution at 0.1 s on a coarse mesh.

Conclusion

- 1 Onelab is an exploring tool and a test platform with a flexible and highly customisable implementation allowing new features to be implemented
- 2 However, it requires skills in numerical analysis and a sound knowledge of Finite Element Method to benefit from the full potential of the solver GetDP
- 3 Underlying theory: de Rham's cohomology. Even though the theory is relatively complex, only general concepts are enough to handle nodal and edge elements in Onelab.
- 4 Simple nodal and edge element coupling leads to lower storage and greater numerical efficiency. It is based on the creation of cuts which is probably the most interesting and appealing feature of the software (especially useful in 3D and complex geometries, quite unique feature compared to available open source software and even commercial software)
- 5 One additional feature is the easy coupling with electric circuitry through global quantities
- 6 The solver is being benchmarked against the commercial well-established software in the community COMSOL Multiphysics[®]. We are using existing benchmarks and cases of practical interest (coils and bulks)

References I

- [1] G. Mur, "Edge elements, their advantages and disadvantages," *IEEE Transactions on Magnetics*, vol. 30, pp. 3552–3557, September 1994.
- [2] P. Dular, "The benefits of nodal and edge elements coupling for discretizing global constraints in dual magnetodynamic formulations," *Journal of Computational and Applied Mathematics*, vol. 168, pp. 165–178, 2004.
- [3] A. Bossavit, "Whitney forms: a class of finite elements for three-dimensional computations in electromagnetism," *IEE Proceedings Pt. A*, vol. 135, pp. 493–500, November 1988.
- [4] M. Nakahara, "Geometry, topology and physics," Graduate student series in Physics, CRC Press, 2003.
- [5] C. Geuzaine, *High order hybrid finite element schemes for Maxwell's equations taking thin structures and global quantities into account*.
Phd thesis, Université de Liège, Faculté des Sciences Appliquées, Octobre 2001.
- [6] M. Pellikka, S. Suuriniemi, L. Kettunen, and C. Geuzaine, "Homology and cohomology computation in finite element modeling," *SIAM: Journal on Scientific Computing (SISC)*, vol. 35, no. 5, pp. B1195–B1214, 2013.
- [7] D. Baldomir and P. Hammond, "Geometry of electromagnetic systems," vol. 39 of *Monographs in electrical and electronic engineering*, Oxford Science Publications, 1996.
- [8] P. Dular, A. Genon, J.-Y. Hody, W. Legros, J. Mauhin, A. Nicolet, "Coupling between Edge Finite Elements, Nodal Finite Elements and Boundary Elements for the Calculation of 3-D Eddy Currents," *IEEE Transactions on Magnetics*, vol. 29, pp. 1470–1474, March 1993.
- [9] P. Dular, F. Henrotte, F. Robert, A. Genon, W. Legros, "A generalized source magnetic field calculation method for inductors of any shape," *IEEE Transactions on Magnetics*, vol. 33, pp. 1398–1401, March 1997.
- [10] A. N. P. Dular, W. Legros, "Coupling of local and global quantities in various finite element formulations its application to electrostatics, magnetostatics and magnetodynamics," *IEEE Transactions on Magnetics*, vol. 34, pp. 3078–3081, September 1998.

References II

- [11] E. J. M. Slodicka, "Convergence of the backward euler method for type-ii superconductors," *Journal of Mathematical Analysis and Applications*, vol. 342, no. 2, pp. 1026–1037, 2008.
- [12] O. C. Zienkiewicz, R.L. Taylor, J.Z.Zhu, *The Finite Element Method: Its basis and fundamentals*. Elsevier, 2005.

Additional reading:

- M. Nakahara, *"Geometry, Topology and Physics,"* CRC Press, 2003.
- P.W. Gross and P.R. Kotiuga, *"Electromagnetic theory and Computation, a topological approach,"* Mathematical Sciences research Institute publications, Vol. 48, Cambridge University Press, 2004.

Extra slides

Derivation of Jacobian matrix "in a sloppy way"

Local Ohm's law,

$$\mathbf{e} = \tilde{\rho} \mathbf{j}$$

$$d\mathbf{e} = \tilde{\rho} d\mathbf{j} + \mathbf{j} d\tilde{\rho}$$

For an isotropic material, $\tilde{\rho}$ is a diagonal tensor, $\tilde{\rho} = \rho \mathbb{I}_3$.

$$\frac{d\mathbf{e}}{d\mathbf{j}} = \rho \mathbb{I}_3 + \mathbf{j} \frac{d\rho}{d\mathbf{j}},$$

$$\frac{d\mathbf{e}}{d\mathbf{j}} = \begin{pmatrix} \rho + j_x \frac{\partial \rho}{\partial j_x} & j_x \frac{\partial \rho}{\partial j_y} & j_x \frac{\partial \rho}{\partial j_z} \\ j_y \frac{\partial \rho}{\partial j_x} & \rho + j_y \frac{\partial \rho}{\partial j_y} & j_y \frac{\partial \rho}{\partial j_z} \\ j_z \frac{\partial \rho}{\partial j_x} & j_z \frac{\partial \rho}{\partial j_y} & \rho + j_z \frac{\partial \rho}{\partial j_z} \end{pmatrix}$$

$$j_k \frac{\partial \rho}{\partial j_l} = j_k \frac{\partial \rho}{\partial j} \frac{\partial j}{\partial j_l} = \frac{\partial \rho}{\partial j} \frac{j_k j_l}{j},$$

$$\frac{d\mathbf{e}}{d\mathbf{j}} = \begin{pmatrix} \rho + \frac{1}{j} \frac{\partial \rho}{\partial j} j_x^2 & \frac{1}{j} \frac{\partial \rho}{\partial j} j_x j_y & \frac{1}{j} \frac{\partial \rho}{\partial j} j_x j_z \\ \frac{1}{j} \frac{\partial \rho}{\partial j} j_y j_x & \rho + \frac{1}{j} \frac{\partial \rho}{\partial j} j_y^2 & \frac{1}{j} \frac{\partial \rho}{\partial j} j_y j_z \\ \frac{1}{j} \frac{\partial \rho}{\partial j} j_z j_x & \frac{1}{j} \frac{\partial \rho}{\partial j} j_z j_y & \rho + \frac{1}{j} \frac{\partial \rho}{\partial j} j_z^2 \end{pmatrix}$$

$$\frac{d\mathbf{e}}{d\mathbf{j}} = \rho \mathbb{I}_3 + \frac{1}{j} \frac{\partial \rho}{\partial j} (\mathbf{j}\mathbf{j}^t),$$